Synthesis, emission and molecular orbital studies of luminescent zirconium thiolate complexes. Crystal structure of [Zr(η^5-C$_5$Me$_5$)$_2$-(SBu^n)$_2$]

Vivian Wing-Wah Yam,* Gui-Zhong Qi and Kung-Kai Cheung

Department of Chemistry, The University of Hong Kong, Pokfulam Road, Hong Kong

A series of luminescent zirconium thiolate complexes [Zr(η^5-C$_5$Me$_5$)$_2$(ER)$_2$] (E = S, R = Bu^n, C$_6$H$_4$Bu^t-p, C$_6$H$_4$Cl-p or Ph; E = Se, R = Ph) have been synthesized by the reaction of [Zr(η^5-C$_5$Me$_5$)$_2$Cl$_2$] with NaER, and shown to exhibit rich luminescence behavior. The crystal structure of [Zr(η^5-C$_5$Me$_5$)$_2$(SBu^n)$_2$] has been determined. Fenske–Hall molecular orbital calculations on the zirconium thiolate complexes revealed a thiolate-based HOMO and a LUMO that is mainly composed of zirconium d character.

As an extension of our continuing effort to explore new classes of luminescent complexes, in particular those of transition metal chalcogenides and chalcogenolates,[1] we have explored the class of d^0 metal chalcogenolates. It is believed that the chalcogenolates, being good σ-donor type ligands, together with the good electron-accepting ability of d^0 metal centers, may give rise hopefully, to, low-lying emissive ligand-to-metal charge transfer (LMCT) excited states. Our interest in these excited states stems from the fact that luminescent LMCT excited states are extremely scarce and only a few of them are reported to luminesce in fluid solution. Examples include Re(C$_5$Me$_5$)$_2$,[2a] [Re(dmpe)$_3$]$^{2+}$,[2b] [Sc(C$_5$Me$_5$)$_2$X] (X = Cl or NHPh),[2c–e] [{Ti-(NR′)[O$_2$P(OR)$_2$]$_2$}$_2$] (R = CMe$_3$ or SiMe$_3$; R′ = CMe$_3$ or CMe$_2$Et),[2f] [Ta(C$_5$Me$_5$)X$_4$] (X = Cl or Br),[2g] [Ta(C$_5$Me$_5$)Cl$_3$X] (X = O$_2$CR or O$_3$SMe),[2g] and a systematic class of d^0 imido-metal complexes of the type *cis,mer*-[M(≡NR)X$_3$L$_2$] (M = Ta or Nb; R = C$_6$H$_3$Pr$^i_2$-2,6; X = Cl or Br; L$_2$ = 2 pyridine, 2-dimethoxyethane, 2 tetrahydrofuran or tetramethylethylenedi-amine).[2h] Thus, an exploration into LMCT excited states would represent a challenging area of research. Moreover, since the vast majority of organometallic complexes have metals in low oxidation states, LMCT transitions, if they do occur, would usually do so at very high energies and may not be observable in the visible region of the spectrum. Thus, a series of d^0 zirconium(IV) chalcogenolates have been synthesized and chosen for our study. In addition, although zirconocene complexes have attracted enormous attention in catalytic processes,[3] synthesis[4] and theoretical studies including those of their titanium congeners,[5] there has been no report on the luminescence of zirconocene complexes. Moreover, it is believed that LMCT excitation would produce charge-transfer excited states in which the metal center of the organometallic complex is formally reduced and may be activated to give novel reactivities. Herein are reported the synthesis and luminescence studies of [Zr(η^5-C$_5$Me$_5$)$_2$(ER)$_2$] (E = S, R = Bu^n, C$_6$H$_4$Bu^t-p, C$_6$H$_4$Cl-p or Ph; E = Se, R = Ph). The crystal structure of [Zr(η^5-C$_5$Me$_5$)$_2$(SBu^n)$_2$] was determined. The electronic structures and the nature of the excited states of these luminescent complexes have been studied by Fenske–Hall molecular orbital calculations. The synthesis and characterization of a series of related zirconocene chalcogenolate complexes have been reported.[4a,b,h,i,j]

Results and Discussion

The complexes [Zr(η^5-C$_5$Me$_5$)$_2$(ER)$_2$] (E = S, R = Bu^n **1**, C$_6$H$_4$Cl-p **2**, C$_6$H$_4$Bu^t-p **3** or Ph **4**; E = Se, R = Ph **5**) were prepared by the reaction of [Zr(η^5-C$_5$Me$_5$)$_2$Cl$_2$] with NaER in
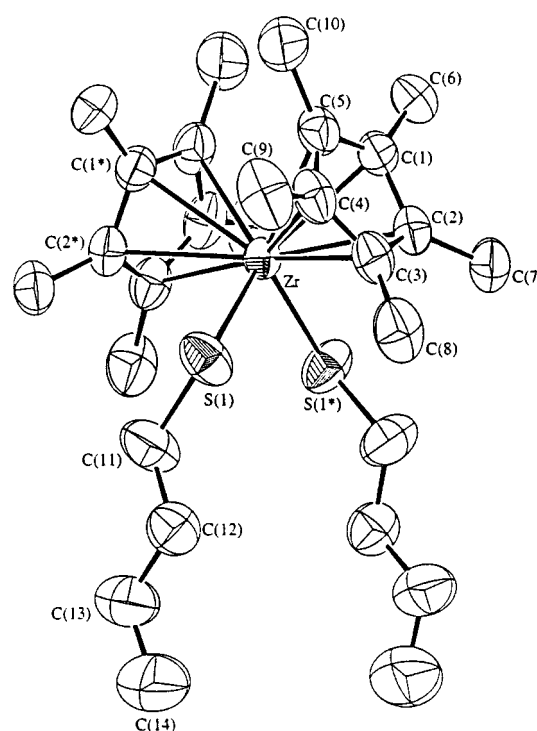

Fig. 1 Perspective drawing of complex **1** with atomic numbering scheme. Thermal ellipsoids are shown at the 50% probability level. Starred atoms have coordinates at 1 − *x*, *y*, 0.5 − *z*

dme at 50 °C for 48 h. Complexes **4** and **5** have been reported previously by Parkin and co-workers[4h] using a different synthetic procedure. All the newly synthesized complexes gave satisfactory elemental analyses. Complexes **1–5** have also been characterized by ^{1}H NMR spectroscopy. The structure of **1** has been determined by X-ray crystallography.

The perspective drawing of complex **1** is depicted in Fig. 1. Selected bond distances and angles are summarized in Table 1. The co-ordination geometry about the Zr atom, defined by the pentamethylcyclopentadienyl ring centroids and the S atoms, is distorted tetrahedral. A projection onto the Zr−S(1)−S(1*) plane shows that the pentamethylcyclopentadienyl rings have a staggered conformation. The Zr−S distance of 2.4987(8) Å is comparable to the values observed in [Zr(η^5-C$_5$Me$_5$)$_2$(SPh)$_2$].[4h] The S(1)−Zr(1)−S(1*) angle of 96.14(5)° is smaller than that of 100.9(1)° observed for [Zr(η^5-C$_5$Me$_5$)$_2$(SPh)$_2$].[4h] This is consistent with the difference in the steric demand of the SBu^n

**Table 1** Selected bond distances (Å) and angles (°) for complex **1**

Zr–S(1)	2.4987(8)	Zr–C(2)	2.593(3)
Zr–C(1)	2.545(3)	Zr–C(4)	2.569(3)
Zr–C(3)	2.606(3)	Zr–Cp*$_{centroid}$	2.27
Zr–C(5)	2.570(3)	C(1)–C(2)	1.410(4)
S(1)–C(11)	1.818(4)	C(3)–C(4)	1.414(4)
C(2)–C(3)	1.412(4)	C(1)–C(5)	1.416(4)
C(4)–C(5)	1.410(4)	C(2)–C(7)	1.505(4)
C(1)–C(6)	1.506(4)	C(4)–C(9)	1.514(4)
C(3)–C(8)	1.505(4)	C(11)–C(12)	1.481(5)
C(5)–C(10)	1.507(4)	C(13)–C(14)	1.441(6)
C(12)–C(13)	1.534(5)		
S(1)–Zr–S(1*)	96.14(5)	Zr–S(1)–C(11)	112.0(1)
S(1)–C(11)–C(12)	112.9(3)	C(11)–C(12)–C(13)	112.2(3)
C(12)–C(13)–C(14)	113.6(4)	Cp*$_{centroid}$–Zr–Cp*$_{centroid}$	135.14

Table 2 Photophysical data for zirconocene chalcogenolate complexes

Compound	Medium (T/K)	Emission λ_{em}/nm
1	Et$_2$O(298)	594
	Light petroleum(77)	596
	Solid(77)	610
	Solid(298)	584
2	Et$_2$O(298)	592
	Light petroleum(77)	572
	Solid(77)	565
	Solid(298)	543
3	Et$_2$O(298)	607
	Light petroleum(77)	576
	Solid(77)	582
	Solid(298)	549
4	Et$_2$O(298)	593
	Light petroleum(298)	591
	thf(298)	594
	Acetone(298)	597
	MeOH(298)	610
	Light petroleum(77)	574
	Solid(77)	578
	Solid(298)	549
5	Solid(77)	594
	Light petroleum(77)	610
6	Solid(77)	660
7	Solid(77)	690
[Zr(η^5-C$_5$Me$_5$)$_2$Cl$_2$]	Solid(77)	494
[Zr(η^5-C$_5$H$_5$)$_2$Cl$_2$]	Solid(77)	452

and SPh moieties. A similar trend has also been observed in the complexes [Ti(η^5-C$_5$H$_5$)$_2$(SEt)$_2$][5c] and [Ti(η^5-C$_5$H$_5$)$_2$(SPh)$_2$].[6] The Zr–Cp*$_{centroid}$ distance of 2.27 Å and the Cp*$_{centroid}$–Zr–Cp*$_{centroid}$ angles of 135.14° are slightly longer and larger, respectively, than that of 2.205 Å and 131° in [Zr(η^5-C$_5$H$_5$)$_2$(SC$_6$H$_4$Cl-*p*)$_2$][4j] consistent with the larger steric bulk of the pentamethylcyclopentadienyl units. An interesting feature worth mentioning is the conformational preference of the thiolate ligands in the Zr(C$_5$Me$_5$)$_2$(SR)$_2$ unit. The conformations may be classified as *endo* (R–S–Zr–S < 90°) or *exo* (R–S–Zr–S > 90°) according to the magnitude of the S–Zr–S–C torsion angle. For **1** the S(1*)–Zr–S(1)–C(11) torsion angle of 48.99° indicates that **1** exhibits an *endo* conformation, which is in accord with theoretical calculations on this class of compounds and is favored by d^0 metal centers in order to maximize the p$_\pi$–d$_\pi$ overlap between sulfur and the metal center.[5] The larger deviation from 90° of the S–Zr–S–C torsion angle in **1** is in line with the steric requirement of the pentamethylcyclopentadienyl units which direct the alkyl substituent further away from the more sterically demanding pentamethylcyclopentadienyl groups. Similar findings have been observed in [Zr(η^5-C$_5$Me$_5$)$_2$(SPh)$_2$].[4h]

The photophysical data of complexes **1–5**, together with those of the related [Zr(η^5-C$_5$H$_5$)$_2$(SC$_6$H$_4$Cl-*p*)$_2$] **6**[4j] and [Zr(η^5-C$_5$H$_5$)$_2$(SC$_6$H$_4$Me-*p*)$_2$] **7**[4j] and the precursor complexes
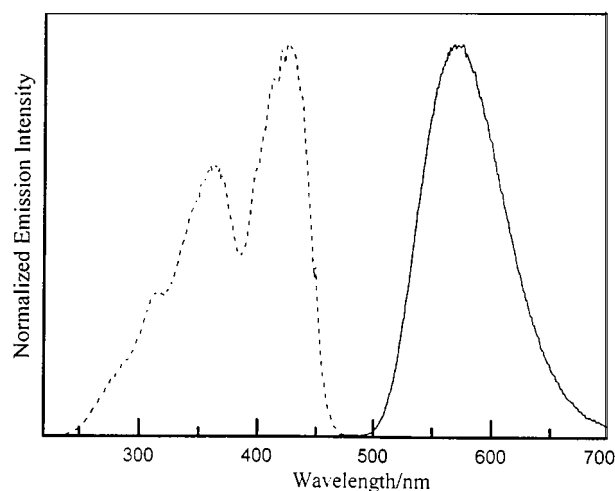
Fig. 2 Excitation (----) and emission spectra (——) of complex **2** in a light petroleum–Et$_2$O (5:1 v/v) glass at 77 K

[Zr(η^5-C$_5$Me$_5$)$_2$Cl$_2$] and [Zr(η^5-C$_5$H$_5$)$_2$Cl$_2$] are collected in Table 2. The excitation and emission spectra of **2** in a light petroleum–Et$_2$O glass at 77 K are shown in Fig. 2. The excitation spectrum closely resembles that of the electronic absorption spectrum. Complexes **1–7** exhibit intense yellow-green to orange-red emission upon visible light excitation in the solid state at 77 K, while [Zr(η^5-C$_5$Me$_5$)$_2$Cl$_2$] and [Zr(η^5-C$_5$H$_5$)$_2$Cl$_2$] emit at 494 and 452 nm, respectively. With reference to previous spectroscopic work on the related titanocene derivatives,[7] it is likely that the emission observed in [Zr(η^5-C$_5$Me$_5$)$_2$Cl$_2$] and [Zr(η^5-C$_5$H$_5$)$_2$Cl$_2$] are derived from the respective C$_5$Me$_5$→Zr and C$_5$H$_5$→Zr ligand-to-metal charge transfer (LMCT) states. The much lower emission emerges in **1–7** relative to their respective [Zr(η^5-C$_5$Me$_5$)$_2$Cl$_2$] and [Zr(η^5-C$_5$H$_5$)$_2$Cl$_2$] counterparts may suggest an emission of different origin. An assignment derived from the C$_5$Me$_5$→Zr and C$_5$H$_5$→Zr LMCT transition, respectively, is not favored since the thiolate and the selenolate ligands being better σ donors than the electronegative chloro group would be expected to render the Zr less electron deficient and hence a poorer electron acceptor. This would cause the C$_5$Me$_5$→Zr and C$_5$H$_5$→Zr LMCT transitions to shift to higher energies. Thus if the emission is derived from such a LMCT state a blue shift in the emission energy should be observed relative to the chloro analogues. The observation of the opposite trend would disfavor such an assignment. A comparison of the emission energies of the complexes in the solid state at 77 K shows that **7** < **6**; **1** < **3** < **4** < **2** and **5** < **4**, in line with the σ-donating effect of the chalcogenolate ligands SC$_6$H$_4$Me-*p* > SC$_6$H$_4$Cl-*p*; SBu^n > SC$_6$H$_4$Bu^t-*p* > SPh > SC$_6$H$_4$Cl-*p* and SePh > SPh, respectively. The observation of such an emission trend is suggestive of either a chalcogenolate to zirconium (ER→Zr) LMCT origin or a chalcogenolate to C$_5$Me$_5$/C$_5$H$_5$ (ER→C$_5$Me$_5$ or ER→C$_5$H$_5$) LLCT origin. The higher emission energy of **2** than that of **6** is in line with both possible assignments since the co-ordination of the more electron-rich C$_5$Me$_5$ on Zr in **2** would render the Zr a poorer electron acceptor and hence a higher LMCT transition energy would result. Similarly, the C$_5$Me$_5$ is a poorer π-acceptor ligand than C$_5$H$_5$, resulting in a higher LLCT transition energy. Although one cannot exclude the possibility of a LLCT state, we prefer an origin with predominant LMCT character since the emission energies appear to be sensitive to the nature of the metal. It is interesting that complexes **6** and **7** are extremely moisture sensitive. If the samples were not freshly prepared for measurements the emission intensity at *ca.* 660–690 nm decreased concomitant with the appearance of a higher-energy emission band typical of the hydrolysed product [{Zr(η^5-C$_5$H$_5$)$_2$(SR)}$_2$O].

In order to provide further insights into the origin of the
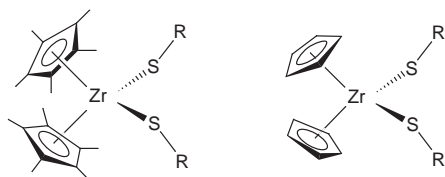
Scheme 1

emission, a Fenske–Hall molecular orbital calculation study was pursued. Table 3 summarizes the idealized bond lengths and angles used for the non-parameterized calculations. The relative positions of the two S atoms and the two C_5Me_5/C_5H_5 rings for $[Zr(\eta^5\text{-}C_5Me_5)_2(SBu^n)_2]$ (two C_5Me_5 rings staggered) and $[Zr(\eta^5\text{-}C_5H_5)_2(SC_6H_4Cl\text{-}p)_2]$ (two C_5H_5 rings eclipsed) are shown in Scheme 1. Table 4 shows the percentage composition for the frontier molecular orbitals of the model complex $[Zr(\eta^5\text{-}C_5Me_5)_2(SBu^n)_2]$ and $[Zr(\eta^5\text{-}C_5H_5)_2(SC_6H_4Cl\text{-}p)_2]$. The results for $[Zr(\eta^5\text{-}C_5Me_5)_2(SBu^n)_2]$ show that the composition of the HOMO is approximately 79% SBu^n and 20% C_5Me_5 in character, while that of the LUMO is approximately 72% Zr and 10% C_5Me_5. On the other hand, for $[Zr(\eta^5\text{-}C_5H_5)_2(SC_6H_4Cl\text{-}p)_2]$, the composition of the HOMO is approximately 95% thiolate ligand in character and that of the LUMO is approximately 65% Zr. The larger cyclopentadienyl orbital contribution in the HOMO of **1** than **6** is in line with the stronger electron-donating property of C_5Me_5 than C_5H_5. The large percentage thiolate character in the HOMO has also been found in the related $[Ti(\eta^5\text{-}C_5H_5)_2(SH)_2]$ based on the structure of $[Ti(\eta^5\text{-}C_5H_5)_2(SPh)_2]$.[8] Based on the results of the calculations, we favor an assignment of the emission as derived from a mixed LMCT state with a predominant thiolate-to-zirconium (RS→Zr) contribution with some C_5Me_5→Zr LMCT contribution in $[Zr(\eta^5\text{-}C_5Me_5)_2(SR)_2]$, and a predominant thiolate-to-zirconium (RS→Zr) LMCT state mixed with some thiolate-to-cyclopentadienyl (RS→C_5H_5) LLCT character in $[Zr(\eta^5\text{-}C_5H_5)_2(SR)_2]$. Such assignments are consistent with the relative σ-donating and π-accepting abilities of C_5Me_5 versus C_5H_5 ligands, the good σ-donating properties of the thiolate ligands, and the trends observed in the emission studies. A similar result has also been reported for $[Ti(\eta^5\text{-}C_5H_5)_2I_2]$ based on MO calculations,[7] where the lowest-energy charge transfer was attributed to I→Ti LMCT transition. This is understandable in view of the fact that the electronegativities of S and I are similar, while for X = F, Cl and Br in $[Ti(\eta^5\text{-}C_5H_5)X_2]$, the lowest-energy charge transfer would be C_5H_5→Ti in nature.

Experimental

Materials and reagents

Bis(pentamethylcyclopentadienyl)zirconium dichloride were from Strem Chemicals, butane-1-thiol, 4-chlorobenzenethiol, 4-*tert*-butylbenzenethiol, benzenethiol and benzeneselenol from Lancaster Synthesis. Analytical grade toluene, 1,2-dimethoxyethane and hexane were dried over sodium and distilled over sodium–benzophenone using standard procedures before use.

Synthesis of zirconium chalcogenolate complexes

All reactions and manipulations were carried out under strictly anaerobic and anhydrous conditions using standard Schlenk techniques.

$[Zr(\eta^5\text{-}C_5Me_5)_2(SBu^n)_2]$ **1.** To a solution of $[Zr(\eta^5\text{-}C_5Me_5)_2Cl_2]$ (0.12 g, 0.28 mmol) in dme (10 cm³) was added $NaSBu^n$ (0.97 mmol) in dme (30 cm³), prepared *in situ* from $HSBu^n$ (0.1 cm³, 0.97 mmol) and an excess of Na, and the reaction mixture was stirred at 50 °C for 48 h. After removal of the solvent under reduced pressure, the solid residue was extracted with toluene. The toluene extract was subsequently concentrated and addition of hexane followed by cooling gave complex **1** as yellow crystals. Yield 0.09 g (62%). ¹H NMR (300 MHz, C_6D_6, 298 K, relative to $SiMe_4$): δ 1.00 (t, 6 H, CH_3), 1.58 (m, 4 H, CH_2), 1.78 (m, 4 H, CH_2), 3.07 (t, 4 H, CH_2S) and 2.05 (s, 30 H, C_5Me_5). UV/VIS in Et_2O (298 K): λ_{max}/nm(ε_{max}/dm³ mol⁻¹ cm⁻¹) 348(4700) and 400(3300) (Found: C, 62.23; H, 8.87. Calc. for $C_{28}H_{48}S_2Zr$: C, 62.31; H, 8.90%).

$[Zr(\eta^5\text{-}C_5Me_5)_2(SC_6H_4Cl\text{-}p)_2]$ **2.** The procedure was similar to that for complex **1** except $HSC_6H_4Cl\text{-}p$ (0.14 g, 0.97 mmol) was used in place of $HSBu^n$ to give **2** as yellow microcrystals. Yield 0.13 g (72%). ¹H NMR (300 MHz, C_6D_6, 298 K, relative to $SiMe_4$): δ 1.78 (s, 30 H, C_5Me_5), 6.90 (d, $J = 8$, 4 H, aryl protons *meta* to S) and 7.56 (d, $J = 8$ Hz, 4 H, aryl protons *ortho* to S). UV/VIS in Et_2O (298 K): λ_{max}/nm(ε_{max}/dm³ mol⁻¹ cm⁻¹) 312(12 200), 354(8560) and 424(5950) (Found: C, 59.49; H, 5.98. Calc. for $C_{32}H_{38}Cl_2S_2Zr$: C, 59.24; H, 5.86%).

$[Zr(\eta^5\text{-}C_5Me_5)_2(SC_6H_4Bu^t\text{-}p)_2]$ **3.** The procedure was similar to that for complex **1** except $HSC_6H_4Bu^t\text{-}p$ (0.16 g, 0.97 mmol) was used in place of $HSBu^n$ to give **3** as yellow microcrystals. Yield 0.11 g (58%). ¹H NMR (300 MHz, C_6D_6, 298 K, relative to $SiMe_4$): δ 1.15 (s, 18 H, Bu^t), 1.92 (s, 30 H, C_5Me_5), 7.03 (d, $J = 8$, 4 H, aryl protons *meta* to S) and 7.83 (d, $J = 8$ Hz, 4 H, aryl protons *ortho* to S). UV/VIS in Et_2O (298 K): λ_{max}/nm(ε_{max}/dm³ mol⁻¹ cm⁻¹) 314(10 300), 356(8630) and 426(6360) (Found: C, 69.34; H, 8.47. Calc. for $C_{40}H_{56}S_2Zr$: C, 69.44; H, 8.10%).

$[Zr(\eta^5\text{-}C_5Me_5)_2(SPh)_2]$ **4.** This complex was prepared by a procedure different from that reported previously.[4h] It was simi-

Table 3 Idealized bond lengths (Å) and angles (°) used for non-parameterized Fenske–Hall MO calculations

Molecule	$[Zr(C_5Me_5)_2(SBu^n)_2]$	$[Zr(C_5H_5)_2(SC_6H_4Cl\text{-}p)_2]$ *
Zr–C_5Me_5/C_5H_5	2.27	2.21
Zr–S	2.50	2.52
S–C	1.82	1.78
C_5Me_5–Zr–C_5Me_5/C_5H_5–Zr–C_5H_5	135.14	131.0
S–Zr–S	96.14	98.95
Zr–S–$C(Bu^n)/Zr$–S–$C(Ph)$	112.0	109.6

* From ref. 4(*j*).

Table 4 Energies and percentage compositions for the frontier orbitals of $[Zr(\eta^5\text{-}C_5Me_5)_2(SBu^n)_2]$ and $[Zr(\eta^5\text{-}C_5H_5)_2(SC_6H_4Cl\text{-}p)_2]$

Complex	Molecular orbital	Energy/eV	% Composition		
			SR	Zr	C_5Me_5/C_5H_5
$[Zr(\eta^5\text{-}C_5Me_5)_2(SBu^n)_2]$	HOMO(88)	−9.38	79.3	0.8	19.9
	LUMO(89)	−3.41	18.9	71.5	9.6
$[Zr(\eta^5\text{-}C_5H_5)_2(SC_6H_4Cl\text{-}p)_2]$	HOMO(68)	−10.00	95.2	0.9	3.9
	LUMO(69)	−4.05	25.0	65.0	10.0

eV ≈ 1.60×10^{-19} J.

lar to that for complex **1** except HSPh (0.11 g, 0.97 mmol) was used in place of HSBu^n to give **4** as orange-yellow crystals. Yield 0.11 g (69%). The ^{1}H NMR data are in agreement with literature values.[4h] UV/VIS: (Et$_2$O, 298 K) λ_{max}/nm(ε_{max}/dm^3 mol^{-1} cm^{-1}): 312(10 200), 354(8210), 424(6180); [light petroleum (b.p. 40–60 °C), 298 K] 312(10 300), 354(8600), 424(6610); (thf, 298 K) 312(8840), 354(7100), 424(5480); (acetone, 298 K) 354(7080), 424(5140); (MeOH, 298 K) 312(9060), 354(6930) and 424(5020).

[Zr(η^5-C$_5$Me$_5$)$_2$(SePh)$_2$] 5. This complex was prepared by a procedure different from that reported previously.[4h] It was similar to that for **1** except HSePh (0.15 g, 0.97 mmol) was used in place of HSBu^n to give **5** as yellow microcrystals. Yield 0.09 g (48%). ^{1}H NMR data are in agreement with literature values.[4h] UV/VIS in Et$_2$O (298 K): λ_{max}/nm(ε_{max}/dm^3 mol^{-1} cm^{-1}) 326(6380), 364(6810) and 446(6250).

Physical measurements and instrumentation

The UV/VIS spectra were obtained on a Hewlett-Packard 8452A diode-array spectrophotometer, steady-state excitation and emission spectra on a Spex Fluorolog 111 spectrofluorometer equipped with a Hamamatsu R-928 photomultiplier tube detector; low-temperature (77 K) spectra were recorded by using an optical Dewar sample holder. Proton NMR spectra were recorded on a Bruker DPX300 Fourier-transform spectrometer. Chemical shifts are reported relative to tetramethylsilane.

Crystallography

Crystal data for complex 1. C$_{28}$H$_{48}$S$_2$Zr, M_r = 540.03, monoclinic, space group $C2/c$ (no. 15), a = 14.847(3), b = 13.234(5), c = 16.394(3) Å, β = 115.96(1)°, U = 2896(1) Å^3, Z = 4, D_c = 1.238 g cm^{-3}, μ(Mo-Kα) = 5.36 cm^{-1}, $F(000)$ = 1152, T = 301 K.

A yellow crystal of dimensions 0.25 × 0.20 × 0.40 mm mounted inside a glass capillary was used for data collection at 28 °C on a Rigaku AFC7R diffractometer with graphite-monochromatized Mo-Kα radiation (λ = 0.710 73 Å) using ω–2θ scans with ω-scan angle (0.73 + 0.35 tan θ)° at a scan speed of 16.0° min^{-1} [up to six scans for reflections I < 15$\sigma(I)$]. Intensity data (in the range $2\theta_{max}$ = 50°; h 0 to 17, k 0 to 15, l −17 to 17 and three standard reflections measured after every 300 showed decay of 3.00%) were corrected for decay and for Lorentz-polarization effects, and empirical absorption corrections were made based on the ψ scan of four strong reflections (minimum and maximum transmission factors 0.981 and 1.000). 2777 Reflections were measured, of which 2666 were unique and R_{int} = 0.012. 2147 Reflections with I > 3$\sigma(I)$ were considered observed and used in the structural analysis. The space group was determined from systematic absences, a statistical analysis of intensity distribution and the successful solution and refinement of the structure solved by direct methods (SIR 92)[9a] and expanded by Fourier techniques and refinement by full-matrix least squares using TEXSAN[9b] on a Silicon Graphics Indy computer. One crystallographic asymmetric unit consists of half the molecule with the Zr atom at a special position. In the least-squares refinement all 16 non-H atoms were refined anisotropically and the 24 H atoms at calculated positions with thermal parameters equal to 1.3 times those of the attached C atoms were not refined. Convergence for 141 variable parameters by least-squares refinement on F with w = $4F_o{}^2/\sigma^2(F_o{}^2)$, where $\sigma^2(F_o{}^2)$ = $\sigma^2(I)$ + (0.024 $F_o{}^2$)^2 for 2147 reflections with I > 3$\sigma(I)$ was reached at R = 0.031 and R' = 0.039 with a goodness of fit of 1.65; $(\Delta/\sigma)_{max}$ = 0.001. The final Fourier-difference map was featureless, with maximum positive and negative peaks of 0.35 and 0.29 e Å^{-3} respectively. Refinement of the enantiomorph led to a higher R of 0.032.

CCDC reference number 186/947.

See http://www.rsc.org/suppdata/dt/1998/1819/ for crystallographic files in .cif format.

Computational details

Non-parameterized Fenske–Hall MO calculations[10] were carried out on the complexes [Zr(η^5-C$_5$Me$_5$)$_2$(SBu^n)$_2$] and [Zr(η^5-C$_5$H$_5$)$_2$(SC$_6$H$_4$Cl-p)$_2$]. This method is based on a self-consistent field method, which is an approximation of the Hartree–Fock–Roothaan procedure. The molecular geometry and the atomic basis sets used completely determine the resulting eigenvalues and eigenvectors. The idealized bond lengths and angles used, summarized in Table 3, were based upon crystallographic data of [Zr(η^5-C$_5$Me$_5$)$_2$(SBu^n)$_2$] and [Zr(η^5-C$_5$H$_5$)$_2$(SC$_6$H$_4$Cl-p)$_2$].[4j] The relative positions of the two S atoms and the two centroids of C$_5$Me$_5$/C$_5$H$_5$ were adjusted to an idealized microsymmetry of C_s (C_1 for overall symmetry) for [Zr(η^5-C$_5$Me$_5$)$_2$(SBu^n)$_2$] (two C$_5$Me$_5$ rings staggered), and C_{2v} (C_2 for overall symmetry) for [Zr(η^5-C$_5$H$_5$)$_2$(SC$_6$H$_4$Cl-p)$_2$] (two C$_5$H$_5$ rings eclipsed) (Scheme 1). The idealized atomic coordinates were taken such that the x direction of the master coordinate system originating on the Zr atom bisects the S–Zr–S bond angle, the y direction is normal to the ZrS$_2$ plane, and the z direction normal to the plane which bisects the S–Zr–S angle. The basis sets used were those provided with the Fenske–Hall program package Version 5.1. All calculations were carried out on a VAX 780 computer at the University of Hong Kong.

Acknowledgements

References

1 See, for example, V. W.-W. Yam, W. K. Lee and T. F. Lai, *J. Chem. Soc., Chem. Commun.*, 1993, 1571; V. W.-W. Yam, K. K. W. Lo and K. K. Cheung, *Inorg. Chem.*, 1996, **35**, 3549; V. W.-W. Yam, K. K. W. Lo, C. R. Wang and K. K. Cheung, *Inorg. Chem.*, 1996, **35**, 5116; V. W.-W. Yam. P. K. Y. Yeung and K. K. Cheung, *J. Chem. Soc., Dalton Trans.*, 1994, 2587; *J. Chem. Soc., Chem. Commun.*, 1995, 267; *Angew. Chem., Int. Ed. Engl.*, 1996, **35**, 739; V. W.-W. Yam. C. L. Chan, K. K. Cheung, *J. Chem. Soc., Dalton Trans.*, 1996, 4019; V. W.-W. Yam, K. M. C. Wong and K. K. Cheung, *Organometallics*, 1997, **16**, 1729; V. W.-W. Yam, *J. Photochem. Photobiol. A*, 1997, **106**, 75; V. W.-W. Yam, K. K. W. Lo, C. R. Wang and K. K. Cheung, *J. Phys. Chem. A*, 1997, **101**, 4666; V. W.-W. Yam and K. K. W. Lo, *Comments Inorg. Chem.*, 1997, **19**, 209.
2 See, for example, (*a*) J. A. Bandy, F. G. N. Cloke, G. Cooper, J. P. Day, R. B. Girling, R. G. Graham, J. C. Green, R. Grinter and R. N. Perutz, *J. Am. Chem. Soc.*, 1988, **110**, 5039; (*b*) Y. F. Lee and J. R. Kirchhoff, *J. Am. Chem. Soc.*, 1994, **116**, 3599; (*c*) B. W. Pfennig, M. E. Thompson and A. B. Bocarsly, *J. Am. Chem. Soc.*, 1989, **111**, 8947; (*d*) B. W. Pfennig, M. E. Thompson and A. B. Bocarsly, *Organometallics*, 1993, **12**, 649; (*e*) A. Jr. Vlcek, *Chemtracts: Inorg. Chem.*, 1993, **5**, 141; (*f*) D. L. Thorn and R. L. Harlow, *Inorg. Chem.*, 1992, **31**, 3917; (*g*) S. Paulson, B. P. Sullivan and J. V. Caspar, *J. Am. Chem. Soc.*, 1992, **114**, 6905; (*h*) K. S. Heinselman and M. D. Hopkins, *J. Am. Chem. Soc.*, 1995, **117**, 12340.
3 See, for example, W. Kaminsky and H. Sinn (Editors), *Transition Metals and Organometallics as Catalysts for Olefin Polymerization*, Springer, Berlin, 1988; R. P. Quirk (Editor), *Transition Metal Catalyzed Polymerizations; Ziegler-Natta and Metathesis Polymerizations*, Cambridge University Press, Cambridge, 1988; Q. Wang, R. Quyoum, D. J. Gillis, M. J. Tudoret, D. Jeremic, B. K. Hunter and M. C. Baird, *Organometallics*, 1996, **15**, 693; B. A. Arndtsen, R. G. Bergman, T. A. Mobley and T. H. Peterson, *Acc. Chem. Res.*, 1995, **28**, 154; T. Imori, V. Lu, H. Cai and T. D. Tilley, *J. Am. Chem. Soc.*, 1995, **117**, 9931; C. P. Schaller, J. B. Bonanno and P. T. Wolczanski, *J. Am. Chem. Soc.*, 1994, **116**, 4133; A. D. Horton, J. de With, A. J. van der Linden and H. van de Weg, *Organometallics*, 1996, **15**, 2672; M. L. H. Green and N. Ishihara, *J. Chem. Soc., Dalton Trans.*, 1994, 657.
4 See, for example; (*a*) H. Köpf, *J. Organomet. Chem.*, 1968, **14**, 353; (*b*) H. Köpf and Th. Klapötke, *Z. Naturforsch., Teil B*, 1985,

40, 1338; (*c*) A. Shaver and J. McCall, *Organometallics*, 1984, **3**, 1823; (*d*) W. A. Howard and G. Parkin, *J. Am. Chem. Soc.*, 1994, **116**, 606; (*e*) M. J. Carney, P. J. Walsh and R. G. Bergman, *J. Am. Chem. Soc.*, 1990, **112**, 6426; (*f*) M. J. Carney, P. J. Walsh, F. J. Hollander and R. G. Bergman, *Organometallics*, 1992, **11**, 761; (*g*) E. Hey-Hawkins, *Chem. Rev.*, 1994, **94**, 1661; (*h*) W. A. Howard, T. M. Trnka and G. Parkin, *Inorg. Chem.*, 1995, **34**, 5900; (*i*) D. W. Stephen and T. T. Nadasdi, *Coord. Chem. Rev.*, 1996, **147**, 147; (*j*) V. W.-W. Yam, G. Z. Qi and K. K. Cheung, *J. Organomet. Chem.*, 1997, **548**, 289.

5 See, for example; (*a*) M. Y. Darensbourg, M. Pala, S. A. Houliston, K. P. Kidwell, D. Spencer, S. S. Chojnacki and J. H. Reibenspies, *Inorg. Chem.*, 1992, **31**, 1487; (*b*) M. A. A. F. d. C. T. Carrondo, P. M. Matias and G. A. Jeffrey, *Acta Crystallogr., Sect. C*, 1984, **40**, 932; (*c*) M. J. Calhorda, M. A. A. F. d. C. T. Carrondo, A. R. Dias, C. F. Frazao, M. B. Hursthouse, J. A. M. Simoes and C. Teixeira, *Inorg. Chem.*, 1988, **27**, 2513; (*d*) M. Y. Darensbourg, C. J. Bischoff, S. A Houliston, M. Pala and J. Reibenspies, *J. Am. Chem. Soc.*, 1990, **112**, 6905; (*e*) J. W. Lauher and R. Hoffmann, *J. Am. Chem. Soc.*, 1976, **98**, 1729; (*f*) J. L. Petersen, *J. Organomet. Chem.*, 1979,

166, 179; (*g*) L. Zhu and N. M. Kostic, *J. Organomet. Chem.*, 1987, **335**, 395.

6 E. G. Muller, S. F. Watkins and L. F Dahl, *J. Organomet. Chem.*, 1976, **111**, 73.

7 See, for example; J. W. Kenney, III, D. R. Boone, D. R. Striplin, Y. H. Chen and K. B. Hamar, *Organometallics*, 1993, **12**, 3671; M. R. M. Bruce, A. Sclafani and D. R. Tyler, *Inorg. Chem.*, 1986, **25**, 2546; M. R. M. Bruce, A. Kenter and D. R. Tyler, *J. Am. Chem. Soc.*, 1984, **106**, 639.

8 J. L. Petersen, D. L. Lichtenberger, R. F. Fenske and L. F. Dahl, *J. Am. Chem. Soc.*, 1975, **97**, 6433.

9 (*a*) SIR 92; A. Altomare, M. Cascarano, C. Giacovazzo, A. Guagliardi, M. C. Burla, G. Polidori and M. Camalli, *J. Appl. Crystallogr.*, 1994, **27**, 435; (*b*) TEXSAN; Crystal Structure Analysis Package, Molecular Structure Corporation, Houston, TX, 1985 and 1992.

10 M. B. Hall and R. F. Fenske, *Inorg. Chem.*, 1972, **11**, 768.